Predicting forest carbon stocks from high resolution satellite data in dry forests of Zimbabwe: exploring the effect of the red-edge band in forest carbon stocks estimation

Tawanda Winmore Gara, Amon Murwira & Henry Ndaimani

Taylor & Francis
Taylor & Francis Group

Predicting forest carbon stocks from high resolution satellite data in dry forests of Zimbabwe: exploring the effect of the red-edge band in forest carbon stocks estimation

Tawanda Winmore Gara[a,b]*, Amon Murwira[a] and Henry Ndaimani[a]

[a]Department of Geography and Environmental Science, University of Zimbabwe, Harare, Zimbabwe; [b]Faculty of Geo-information Science and Earth Observation (ITC), Enschede, The Netherlands

In this study, we tested whether the inclusion of the red-edge band as a covariate to vegetation indices improves the predictive accuracy in forest carbon estimation and mapping in savanna dry forests of Zimbabwe. Initially, we tested whether and to what extent vegetation indices (simple ratio SR, soil-adjusted vegetation index and normalized difference vegetation index) derived from high spatial resolution satellite imagery (WorldView-2) predict forest carbon stocks. Next, we tested whether inclusion of reflectance in the red-edge band as a covariate to vegetation indices improve the model's accuracy in forest carbon prediction. We used simple regression analysis to determine the nature and the strength of the relationship between forest carbon stocks and remotely sensed vegetation indices. We then used multiple regression analysis to determine whether integrating vegetation indices and reflection in the red-edge band improve forest carbon prediction. Next, we mapped the spatial variation in forest carbon stocks using the best regression model relating forest carbon stocks to remotely sensed vegetation indices and reflection in the red-edge band. Our results showed that vegetation indices alone as an explanatory variable significantly ($p < 0.05$) predicted forest carbon stocks with R^2 ranging between 45 and 63% and RMSE ranging from 10.3 to 12.9%. However, when the reflectance in the red-edge band was included in the regression models the explained variance increased to between 68 and 70% with the RMSE ranging between 9.56 and 10.1%. A combination of SR and reflectance in the red edge produced the best predictor of forest carbon stocks. We concluded that integrating vegetation indices and reflectance in the red-edge band derived from high spatial resolution can be successfully used to estimate forest carbon in dry forests with minimal error.

Keywords: forest carbon stocks; vegetation indices; red-edge band; high spatial resolution satellite imagery; dry forests; savanna woodlands

1. Introduction

Terrestrial ecosystems play an important role in understanding biosphere–atmosphere interactions especially the global carbon cycling. Increased emissions of greenhouse gases particularly carbon dioxide in the atmosphere are responsible for global warming and climate change. Carbon sequestration by terrestrial ecosystems particularly forests is considered an important pathway to mitigate the greenhouse effect and climate change (Gibbs et al. 2007). In this context, measurement of forest characteristics such

---

*Corresponding author. Email: t.w.gara@utwente.nl

as carbon stocks is important in fulfilling the requirements of the United Nations Framework Convention on Climate Change, particularly the Kyoto Protocol and the Reducing Emissions from Deforestation and Forest Degradation (REDD+) initiative. The Kyoto Protocol advocates for measuring and monitoring carbon stocks in terrestrial vegetation based on the knowledge that changes in the forest carbon stocks influences concentrations of atmospheric carbon dioxide (Zianis et al. 2005). The REDD+ initiative aims at reducing emissions from ecosystem degradation and deforestation by enhancing forest conservation and enhancement of carbon stocks through sustainable utilization of forest resources. However, the contribution of dry forests, particularly the African savanna woodlands to the global carbon cycle, is little understood (Williams et al. 2007). Thus, the development of methods for understanding the contribution of savanna dry forests in the global carbon cycle is critical for dry forest conservation and enhancement of carbon stocks in these ecosystems (Gara et al. 2014). Such methods may need to focus on improving the estimates of forest carbon stocks in savanna dry forest.

Although field measurements are regarded as the most accurate method of estimating forest carbon stocks (De Gier 2003; Lu 2006), these measurements are costly and labour intensive and can only be feasible over smaller scales (Van et al. 2000; Ketterings et al. 2001; Northup et al. 2005). In this regard, the development of methods that supplement field measurements is important. Among these methods is remote sensing which provides an opportunity to estimate and extrapolate carbon stocks over large spatial extents. The Inter-Governmental Panel on Climate Change Good Practice Guidance (IPCC GPG) on Land Use, Land-use Change and Forestry (IPCC 2003), advocates for the use of remote sensing in forest carbon stocks estimation because of its repeatability, cost effectiveness and synoptic view (Muukkonen & Heiskanen 2005). Remote sensing methods for estimating forest carbon stocks are still few and far between, particularly for dry forests. To this end, the development of remote sensing methods to quantify carbon stocks in dry forests such as savanna woodlands of Southern Africa is important for carbon inventory and reporting (IPCC 2003). However, the level of accuracy and reliability of remote sensing methods principally depends on the ability of a sensor to characterize the spatial and temporal heterogeneity in forest carbon stocks with minimal error. Thus, knowledge on the performance of satellite borne sensors to estimate carbon stocks is critical.

There are known limitations in vegetation indices derived from medium to low spatial resolution satellite imagery despite their wide application in estimating biomass and forest carbon stocks in various vegetation biomes. Often, models developed from these sensors are associated with high uncertainties and high prediction errors (Cho et al. 2007). Several studies demonstrate weak to average relationships between spectral reflectance signal acquired from medium to low resolution data and above-ground biomass in savanna woodlands (Mutanga & Rugege 2006; Verbesselt et al. 2006; Wessels et al. 2006). For example, Mutanga and Rugege (2006) used a number of vegetation indices derived from MODIS to estimate herbaceous biomass in savanna woodlands and their highest coefficient of determination (R^2) was 44%. On the other hand, Samimi and Kraus (2004) found no significant relation between Landsat spectral vegetation indices and biomass in a study carried out in four study sites in Southern Africa. These limitations and inconsistencies might be attributed to mixed pixels commonly associated with medium to low resolution satellite imagery especially in the African savanna. Mixed pixels result when the sensor receives reflectance signals from alternating earth surface material (bare soils, vegetation or even water) within the same pixel

(Muukkonen & Heiskanen 2007). In addition, it is difficult to match the size of field plots with the spatial resolution of the medium and low sensors. This limits the effectiveness and accuracy of these satellite images (Eisfelder et al. 2011). In this regard, we hypothesize that remote sensing methods that estimate dendrometric characteristics based on improved high spatial resolution sensors (spatial resolution <5 m) are critical to test whether the mapping accuracy of the dendrometric characteristics such as forest carbon can be improved.

The availability of high spatial resolution sensors such as WorldView-2 and RapidEye, together with the inclusion of the red-edge (RE) band (approximately 0.68– 0.75 μm) has provided data that can be used to improve the quantification and mapping of forest carbon stocks at local scales. The red edge is the region or boundary in the spectral profile of healthy vegetation between the chlorophyll absorption red wavelengths and the leaf scattering near-infrared wavelength (Filella & Penuelas 1994). The RE band is sensitive to chlorophyll, leaf area index and biomass (Turpie 2013). However, the application of red edge has mainly been limited to biomass and biochemical analysis (nitrogen) of crop/grass using hyperspectral imagery (Mutanga & Skidmore 2007). The application of the RE band of multispectral satellite imagery in forestry studies is still rudimentary. Moreover, the anticipated advantage of high spatial resolution sensors is in their ability to derive near pure pixels. For example, in landscapes such as savanna woodlands where vegetation distribution is sparse, spatial heterogeneity of forest carbon occurs at short distances. Thus, high spatial resolution data become critical due to its ability to capture uniform and unique pixels, thereby reducing uncertainties in forest carbon estimations at local scales. To date, studies assessing the utility of high spatial resolution satellite imagery for estimating biomass and carbon have focused on moist forests and homogenous plantations. In this context, the utility of multispectral imagery of high spatial resolution such as WorldView-2 and the RE band in estimating and modelling carbon in dry forests especially savanna woodlands of Southern Africa remains to be established (Eisfelder et al. 2011).

In this study, we tested whether, to what extent and in what form vegetation indices (i.e. simple ratio (SR), soil-adjusted vegetation index (SAVI) and normalized difference vegetation index (NDVI) derived from high spatial resolution sensors, i.e. WorldView-2, can predict forest carbon in savanna woodlands of Southern Africa. We also tested whether including reflectance in the RE band as an explanatory variable to vegetation indices can improve the estimation of forest carbon stocks. We used the best predictive model relating forest carbon stocks to remotely sensed vegetation indices and reflectance in the RE band to map the spatial variations in forest carbon stocks in Malipati Safari Area in Zimbabwe.

2. Materials and methods

2.1. Study sites

The study was carried out in Malipati Safari Area in south east Zimbabwe (Figure 1). *Colophospermum mopane* is the dominant tree species in Malipati with *combretum* spp being a codominant tree species. Table 1 details the location as well as the bio-physical and climatic conditions of the study site. The study site was selected because human disturbance is minimal as wood cutting is not allowed in these protected areas. Thus, the relationships between dendrometric characteristics and satellite imagery data are assumed to be less affected by human disturbance.
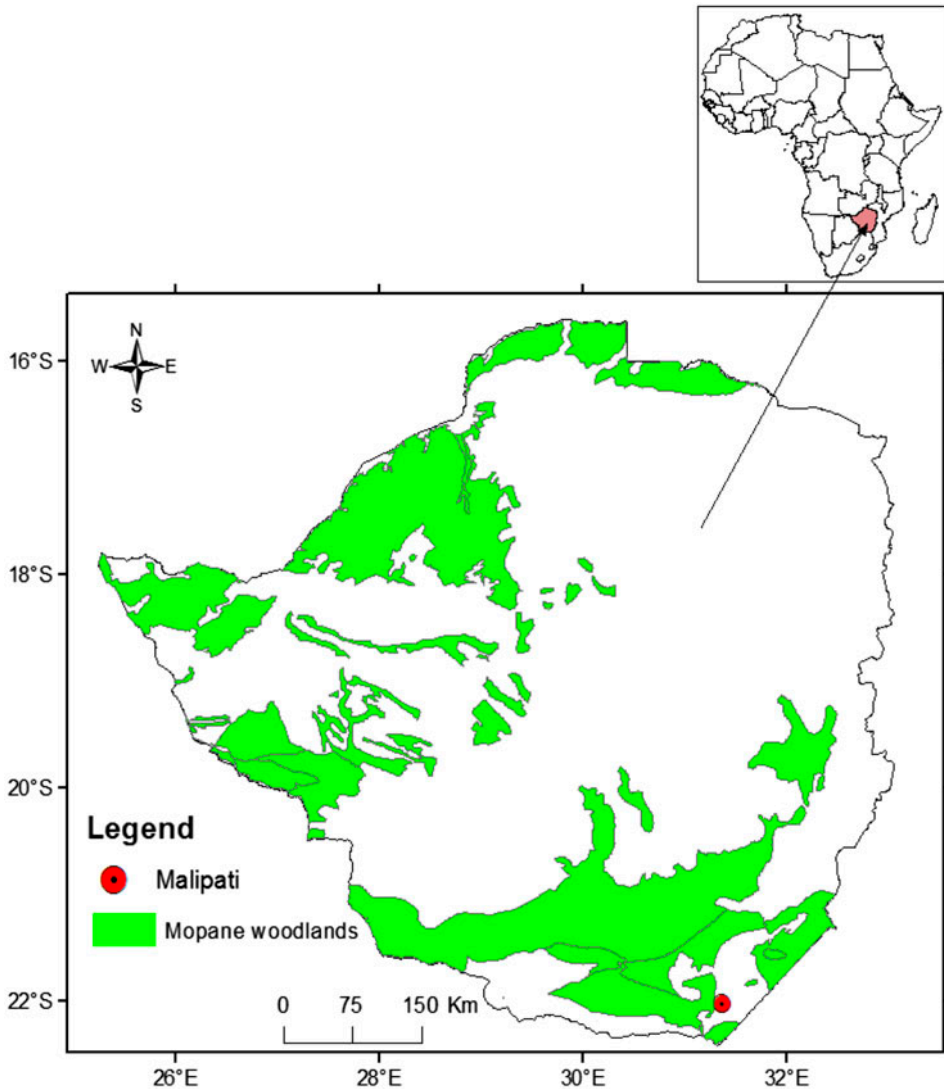
Figure 1.   The location of Zimbabwe (insert) and spatial distribution of *C. mopane* woodlands in Zimbabwe.

2.2.   Sampling design and field measurements

Before field data collection, we classified WorldView-2 of 14 May 2011 for Malipati into three land cover types, i.e. woodland, wooded grassland and bare firstly using the unsupervised iterative self-organizing data analysis technique (ISODATA) algorithm. After clustering using the ISODATA algorithm, we inspected and labelled visually the classified image. We then randomly generated sampling points in woodlands and wooded grasslands in ArcView GIS 3.2 (www.esri.com). Randomly generated points were used as plot centres in the field data collection.

We sampled 37 plots, and we deemed the number large enough for statistical purposes (Rawlings et al. 1998). In the field, we used a hand-held Global Positioning

Table 1. Biophysical and climatic conditions of the study sites.

Characteristics	Malipati
Longitude	31°20′−31°24′E
Latitude	22°01′−22°03′S
Altitude (m)	300–600
Rainfall (mm)	300–600
Rain season	November–March
Temperature range (°C)	5–33
Vegetation type	Mopane
Soil classification	Lithosols and vertisols

System (*Garmin GPSmap 60CSx*) to navigate to the sampling points with an error of ±2 m. We did not correct the accuracy of the GPS as ±2 m was deemed adequate considering the plot size (30 m × 30 m) used in this study. At each random point, a north-oriented plot measuring 30 m × 30 m (0.09 ha) was marked using a tape measure. Plots were oriented to the north using a magnetic compass. The plot size was determined following Rahman et al. (2008) 30 m × 30 m plot size recommendation for primary forests. For each standing tree greater than 10 cm in diameter at breast height (DBH) and 3 m in height (Gschwantner et al. 2009), we identified the tree species and measured DBH (at 1.3 m above ground surface) and total tree height. We first measured stem circumference using a tape measure in the field and later converted it to DBH in a computer spreadsheet. Total tree height was estimated in the following manner: we first used a clinometer to estimate the angle of elevation by aiming at the top and the base of a tree from a measured distance and then calculating the height in a spreadsheet using the trigonometric principle.

2.3. Forest carbon estimation

Forest carbon was estimated from wood volume following a number of computational steps. Firstly, wood volume was estimated from existing allometric equations developed for sites with similar vegetation types, rainfall and temperature. We used allometric equations for individual tree species (Table 2). We then computed wood volume per plot as the sum of the individual tree species volumes. Secondly, following Brown (1997), we then converted wood volume to above-ground biomass (AGB) using the function:

$$AGB(t/\text{ha}) = VOB \times WD \times BEF \qquad (1)$$

where VOB is wood volume over bark estimated from allometric equations, WD is wood density, and BEF is biomass expansion factor. WD and BEF were determined

Table 2. Allometric equation used in the study.

Species	Allometric Equation	References
C. mopane	$V = 0.0001065 \times DBH^{2.471}$	Henry et al. (2011)
Combretum apiculatum	$V = (0.0132 + 0.00079DBH^2 + 0.0103H_t)^2$	Abbot et al. (1997)
Others species	$V = DBH^2/4 * \pi * H_t * \pi * f\text{gross}$	ILUA (2008)

Notes: V, wood volume; DBH, diameter at breast height; BA, basal area; H_t, tree total height; f_{gross}, 0.74.

following Brown ([1997](#)). Finally, we multiplied the above-ground biomass by a conversion ratio of 0.5 to obtain forest carbon (IPCC [2003](#)). This ratio considers that 45–55% of forest aboveground biomass is carbon (Rahman et al. [2008](#)). We then scaled up carbon/plot (30 m × 30 m) to carbon/hectare using plot expansion factor (PEF) using the following formula:

$$\text{PEF} = \frac{10000}{\text{Plotsize (m}^2)} \tag{2}$$

where PEF is plot expansion factor, and the plot size was 900 m^2 (30 m × 30 m).

2.4. Remote sensing data

2.4.1. Image pre-processing

A WorldView-2 satellite image for 14 May 2011 acquired from DigitalGlobe (http://worldview2.digitalglobe.com/) was used in this study. WorldView-2 (2 m spatial resolution) has eight multispectral bands in the spectral range of 400–450 μm (coastal blue), 0.45–0.51 μm (blue), 0.51–0.58 μm (green), 0.585–0.625 μm (yellow), 0.63–0.69 μm (red), 0.705–0.745 μm (red edge), 0.77–0.895 μm (NIR-1) and 0.86–1.040 μm (NIR-2). The Worldview-2 satellite imagery was radiometrically and geometrically corrected before satellite data computation. We converted the WorldView-2 to surface reflectance using QUAC (QUick Atmospheric Correction) (Bernstein et al. [2005b](#)) in ENVI 4.8. The QUAC algorithm establishes atmospheric compensation parameters from the information contained within the scene (observed endmember spectra), thus allowing the retrieval of accurate reflectance values for different earth surface materials. The WorldView-2 image was geometrically corrected to less than a pixel using 10 points measured in the field using a *Garmin GPSmap 60CSx* GPS at a positional error of ±2 m. We applied a first-order polynomial transformation to the WorldView-2 imagery because the study area has a generally even terrain.

2.4.2. Remotely sensed vegetation indices

In this study, we used remotely sensed vegetation indices and reflectance in the RE band to estimate forest carbon using regression analysis. We tested the hypothesis that the inclusion of the RE band as an explanatory variable together with vegetation indices, i.e. SR, NDVI and SAVI derived from high spatial resolution significantly improves forest carbon stocks estimations in African savanna woodlands. To achieve this, we first computed vegetation indices, i.e. SR, NDVI and SAVI (Table [3](#)) based on high spatial resolution satellite imagery, i.e. WorldView-2. In all vegetation indices computations, we used the red spectral band, i.e. 0.63–0.69 μm, and the near-infrared band (NIR-1), i.e. 0.77–0.895 μm. We used NIR-1 band of WorldView-2 of Malipati in vegetation indices computation because NIR-1 derived vegetation indices demonstrated stronger relationship with carbon compared with NIR-2. Since vegetation in the Malipati is generally sparse, we used SAVI due to its minimization of soil background reflectance (Huete [1988](#)). SR and NDVI were also used because they are well documented as good measures of biomass and vegetation vigour (Jordan [1969](#); Tucker [1979](#)). Next, we extracted the reflectance in the RE band and vegetation indices from WorldView-2 imagery per plot using the average of a 15 × 15 pixel (30 m × 30 m) window centred on the GPS location of each field plot.

Table 3. Vegetation indices used in the study.

Vegetation indices	Formula	Reference
Simple ratio	$\frac{\rho\text{NIR}}{\rho R}$	Jordan (1969)
Normalized difference vegetation index	$\frac{\rho\text{NIR} - \rho R}{\rho\text{NIR} + \rho R}$	Tucker (1979)
Soil-adjusted vegetation index	$\left(\frac{\rho\text{NIR} - \rho R}{\rho\text{NIR} + \rho R + L}\right) \times 1 + L$	Huete (1988)

Notes: NIR is reflectance in the near-infrared band, R is reflectance in the Red, $L = 0.5$ (soil correction factor).

2.5. *Relating forest carbon and vegetation indices*

We used simple and multiple regression analysis to examine the nature and strength of relationship between forest carbon stocks, vegetation indices and reflectance in the red-edge band in a statistical software. Prior to regression analysis, we tested the forest carbon data for spatial auto-correlation using *Moran's I* to test for conformity with the least squares regression assumption of randomness (Legendre 1993). We observed that our data were not spatial autocorrelated ($I = 0.01$, $Z = 0.3$, $p > 0.05$). Secondly, we tested if collinearity exists between the explanatory variables, i.e. vegetation indices and reflectance in the RE band using the variance inflation factor (VIF) statistic (Brauner & Shacham 1998). In all cases, the VIF between all the vegetation indices and reflectance in the RE band was less than 10 meaning collinearity did not exist between the explanatory variables (Table 4).

In all regression analyses, forest carbon stock was the dependent variable, while vegetation indices and reflectance in the RE band was the independent variables. We used a linear regression model (model 1) and second order polynomial regression model (model 2) (Tables 4 and 5) to test the relationships between forest carbon and vegetation indices and reflection in the RE band. Initially, we performed regression analysis between forest carbon stocks and vegetation indices. Next, we included the reflectance in the RE band as a explanatory variable to test whether the model performance improves. The validity of each regression model was evaluated based on the root mean square error (RMSE), the coefficient of determination (R^2), the Akaike Information Criterion (AIC) and the level of significance (*p*-value) of the overall model as well as the significance level of the coefficients (slope and intercept). Specifically, in choosing the best fit regression model, we selected a significant model ($p < 0.05$), with the lowest RMSE, highest R^2 and low AIC. The AIC is goodness of fit indicator that penalize a model for increasing number of parameters. Increased number of fitting often results in over parameterization. An optimal model has a low AIC. The AIC is defined as,

$$\text{AIC} = -2^* \ln(\text{likelihood}) + 2^*K$$

Table 4. Correlation matrix of vegetation and the reflectance in the RE band.

	Red edge	NDVI	SAVI
Red edge			
NDVI	0.18		
SAVI	0.43	0.96	
SR	0.13	0.99	0.95

Table 5. Descriptive statistics of field data set for Malipati.

	Min	Max	Mean	SD
Carbon (Mg ha^{-1})	8.77	17	12.88	2.08
DBH (cm)	10.18	30.23	16.33	4.23
Tree density (ha^{-1})	33	522	299	114

Notes: Min, minimum; max, maximum; SD, standard deviation.

where ln is the maximum log-likelihood of the model and K is the number of parameters in the model.

The significance level of the intercept was also considered, and a model with a insignificance ($p > 0.05$) intercept was considered a better model. An insignificant intercept implies that intercept is not significantly different from 0 ($b_1 = 0$). This means such a model does not underestimate or overestimate forest carbon values at low vegetation indices and RE reflectance values. Moreover, for all best fit models, residuals were tested for normality using the *shapiro–wilk* test. We also plotted scatterplots of standardized residuals against fitted values of forest carbon stocks to test for conformity with the least squares regression assumption of homogenous variance (heteroscedasticity).

We used a k-fold cross validation to check the performance of the regression models because our sample size ($n = 37$) was small. A k-fold value of 10 was used in all cross validation analysis. The operation splits the data set into 10 equal partitions. At each iteration, $k-1$ will be used to calibrate the model while the remaining partition is used for validation. This process is repeated iteratively k times until all the segments are used for validation as well for calibration. The k-fold validation output (mean square) was then used to calculate the RMSE and the RMSE% using the following mathematical formula:

$$\text{RMSE} = \sqrt{\frac{1}{n}\sum_{i=1}^{n}(y_i - \hat{y}_i)^2}; \ \text{RMSE}(\%) = \frac{\sqrt{\frac{1}{n}\sum_{1=n}^{n}\left(y_i - \hat{y}_i\right)^2}}{\bar{y}} \times 100 \qquad (3)$$

where y_i is observed carbon, $\hat{y}$ is predicted carbon, $\bar{y}$ is the mean of the observed carbon, n is the number of plots in the test data set.

For mapping the spatial distribution of forest carbon, we used the best regression model to map the spatial distribution of forest carbon stocks in the two study sites. Specifically, we mapped carbon in the study site using regression models which had the highest R^2, the lowest AIC and the lowest RMSE. So for both sites, we use SR models to map spatial variations in forest carbon.

3. Results

3.1. *Field measurement of variables related to forest carbon*

Table 5 shows the descriptive statistics of field data set for Malipati. Tree size was significantly different within and among plots in the study area (Figure 2).
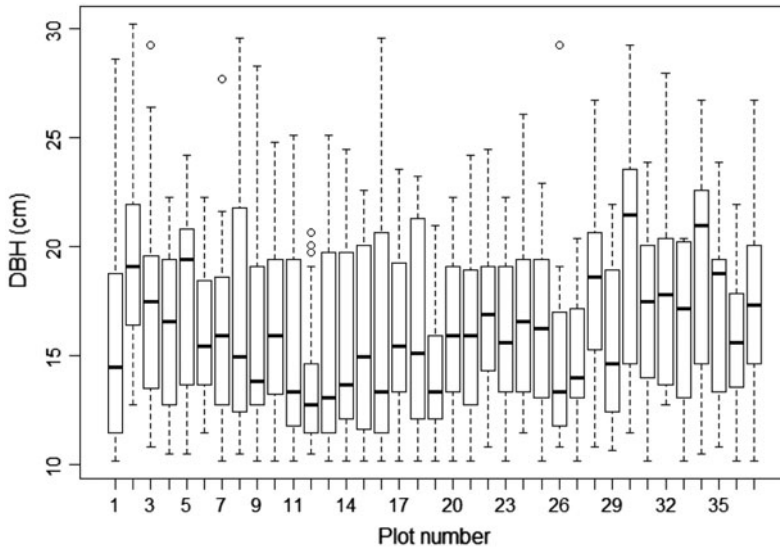
Figure 2.   Variations in tree sizes per plot in Malipati.

3.2.   *Statistical models*

The strength of relationship between carbon stocks and vegetation indices varied with respect to the vegetation index used (Figure 3). All simple regression models using vegetation indices as the only explanatory variable were significant ($p < 0.05$) with a RMSE ranging from 10.3 to 12.9% and AIC values ranging from 132 to 195 (Table 6). Linear models had a low RMSE and AIC values thus characterizing the relationship between vegetation indices and carbon better than the 2nd order polynomial models. The slopes of all linear regression models were positive. In other words, an increase in forest carbon stocks corresponds to an increase in vegetation indices. The intercept (β_0) of all the regression were significant ($p < 0.05$), implying an overestimation and underestimation in positive intercepts and negative intercepts, respectively. All vegetation indices explained more than 50% variation in forest carbon except for SAVI.

By adding reflectance in the red-edge band as an explanatory variable, the R^2 increased and the RMSE and AIC also decreased for all models (Table 7). For example, using simple regression, SAVI alone as an explanatory variable the model explained 45% variance in carbon stocks with a RMSE of 11.9% and an AIC value of 195, however, when the reflectance in the red-edge band was included as an explanatory variable the R^2 rose to 68%, whilst the RMSE and AIC decreased to 9.46 and 127, respectively. However, the intercept (17.91) of the model relating carbon stocks with SAVI and reflectance in the RE was significant different ($p < 0.05$) from 0 intercept ($b_1 \neq 0$) indicating overestimation of forest carbon stocks at low SAVI and RE values. The SR explained 62% variance in carbon stocks when used a single explanatory variable with a RMSE of 10.3% and an AIC of 132. With the inclusion of reflectance in the red edge, the R^2 increased to 68% with a RMSE of 9.56% and an AIC of 127. Likewise, NDVI explained 59% variance in carbon stocks when used a single explanatory variable with a RMSE of 10.3% and an AIC of 132. With the inclusion of reflectance in the red edge, the R^2 increased to 68% with a RMSE of 9.56% and an AIC of 127. The intercept for NDVI and SR models when RE was included as an
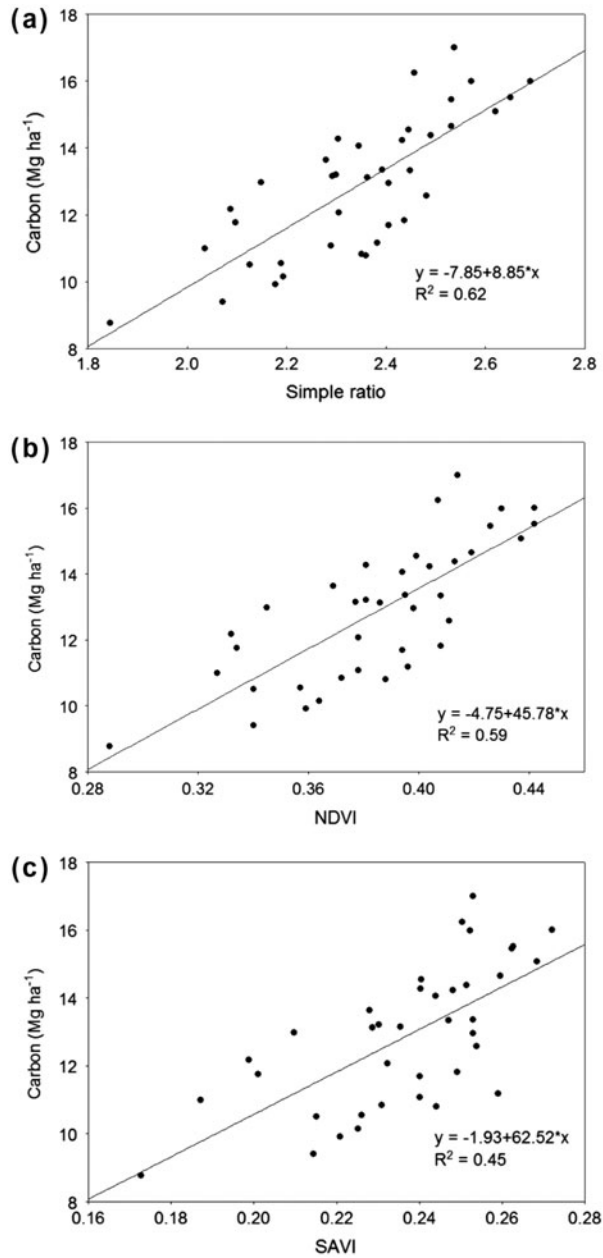
Figure 3. Relationships between forest carbon and vegetation indices (a = SR, b = NDVI, c = SAVI).

explanatory were not significantly ($p > 0.05$) different from 0 ($b = 0$) indicating optimal estimations of carbon stocks at low SR/NDVI and RE values. It is therefore worthwhile to note that SR and NDVI performed relatively better when the reflectance in the red edge was included in the model because the R^2 increased, while the AIC and RMSE dropped and the intercept was not significantly different from 0 (see Figure 4).

Table 6. Regression models with vegetation indices as explanatory variable.

Predictors	Model	Equation	R^2	AIC	RMSE (%)
SR	1	$-7.85 + 8.85$ (SR)	0.62	132	10.3
	2	$16.37 - 12.32$ (SR) $+ 4.56$ (SR^2)	0.63	133	10.4
NDVI	1	$-4.75 + 45.78$ (NDVI)	0.59	134	10.7
	2	$19.8 - 86.2$ (NDVI) $+ 175.7$ (NDVI^2)	0.61	135	10.9
SAVI	1	$-1.93 + 62.52$ (SAVI)	0.45	195	11.9
	2	$22.8 - 158$ (SAVI) $+ 486.3$ (SAVI^2)	0.48	146	12.9

Table 7. Regression models with vegetation indices and the red edge as explanatory variables.

Predictors	Model	Equation	R^2	AIC	RMSE (%)
SR + RE	1	$3.04 + 9.21$ (SR) $- 57.67$ (RE)	0.68	127	9.56
	2	$12.05 - 13.69$ (SR)$+108.33$ (RE) $- 0.21$ (SR^2) $-$ 1077.68 (RE^2) $+ 118.96$ (SR*RE)[a]	0.69	132	9.93
NDVI + RE	1	$7.7 + 48.87$ (NDVI) $- 66.9$ (RE)	0.68	128	9.62
	2	$9.07 - 120.62$ (NDVI) $+ 227.58$ (RE) $+ 18.26$ (NDVI^2) $- 1438.34$ (RE^2) $+ 776.88$ (NDVI*RE)[a]	0.7	133	10.1
SAVI + RE	1	$17.91 + 83.57$ (SAVI) $- 121.75$ (RE)	0.68	127	9.46
	2	$-12.9 - 173.9$ (SAVI) $+ 469.3$ (RE) $+ 104.3$ (SAVI^2) $- 2045.9$ (RE^2) $+ 1045$ (SAVI*RE)[a]	0.69	132	10

Notes: RE: reflectance in the red edge.
[a]Depicts insignificant coefficients (slope and intercept).

The three vegetation indices performed similarly when reflectance from the RE band was included as an explanatory as shown by scatterplots between the measured carbon and carbon predicted from vegetation indices (Figure 5). This is also observed on the similar spread of the predicted vs. measured carbon around the 1:1 line. The spatial distribution of carbon stocks as estimated from SR and reflectance in the RE band is shown in (Figure 6).

4. Discussion

Results in this study indicate that including reflectance in the RE band as an explanatory variable to remotely sensed vegetation indices derived from the WorldView-2 significantly improve forest carbon stocks estimations in dry forests of Zimbabwe. The inclusion of the RE band increased the R^2 and lowered the RMSE and AIC value of all regression models. These results are consistent with our initial hypothesis that the red edge is an important explanatory variable in estimation and modelling forest carbon in savanna dry forests. The RE region is sensitive to parameters of vegetation such as canopy biomass and chlorophyll content that are inherently related to forest carbon stocks (Mutanga et al. 2012). Results obtained in this study are consistent with Cho et al. (2007) who observed improved predictive performance of the red edge extracted from airborne HyMap hyperspectral imagery in estimating grass/herb biomass in the Majella National Park. Thus, from our results, we put forward a claim that integrating reflectance in the RE band and vegetation indices derived high spatial resolution imagery can be used for accurate estimation of forest carbon stocks.
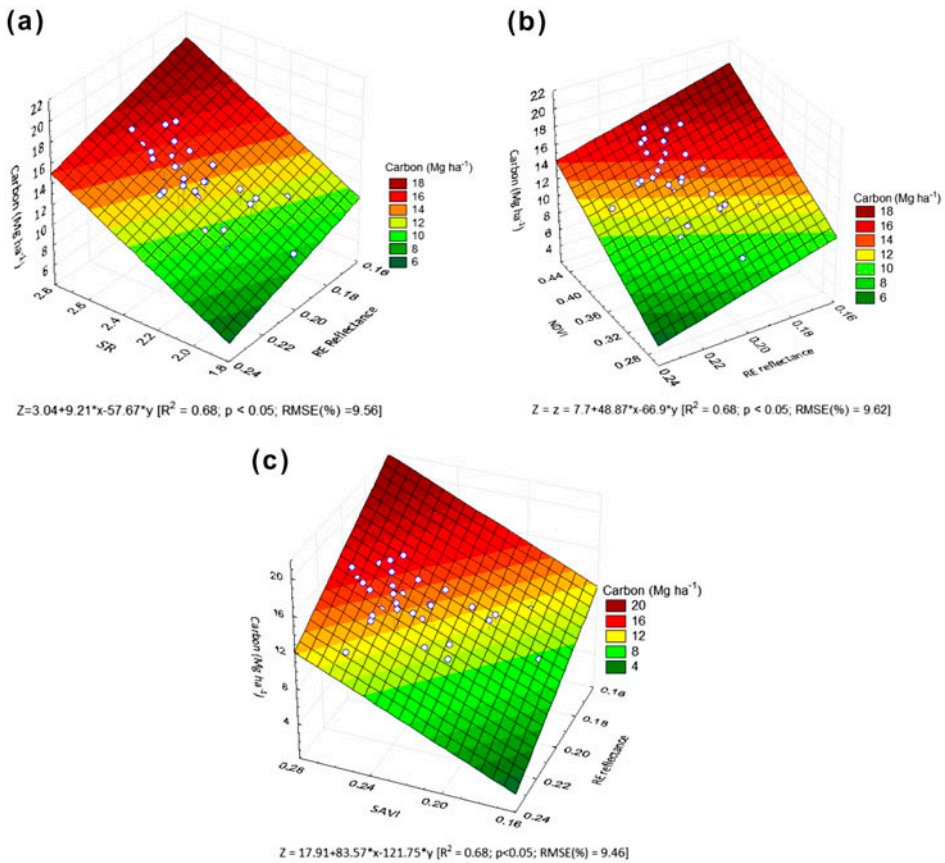
Figure 4. A relationship between forest carbon, vegetation indices (a = SR, b = ND, c = SAVI) and reflectance in the RE band. The graph shows decreasing carbon (high carbon) deep red to low carbon (dark green).

The best model explained 68% variation in forest carbon with a RMSE of 9.56%. This coefficient of determination is higher than obtained by Mutanga and Rugege (2006) and Samimi and Kraus (2004) in the similar ecosystems. Mutanga and Rugege (2006) used a number of vegetation indices derived from MODIS to estimate herbaceous biomass in savanna woodlands in Kruger National Park, South Africa, and their highest coefficient of determination (R^2) was 44%. Samimi and Kraus (2004), on the other hand, found no significant relation between Landsat spectral vegetation indices and biomass in a study carried out in four study sites in Southern Africa. Possible reasons for the difference in results of this study and that of Mutanga and Rugege (2006) and Samimi and Kraus (2004) are that in this study we used vegetation indices derived from high spatial resolution data. We also integrated reflectance in the RE band with conventional vegetation indices and this improved predictions in carbon stocks significantly. It is important to note that although the models performed better than previous studies in the savanna dry forest, the coefficient of determination was not very high (>75%) as we expected. This can be attributed to the fact tree carbon content is a factor of tree height and DBH; however, spectral vegetation indices derived from Worldview-2 can only characterize canopy greenness which is related to DBH. In this
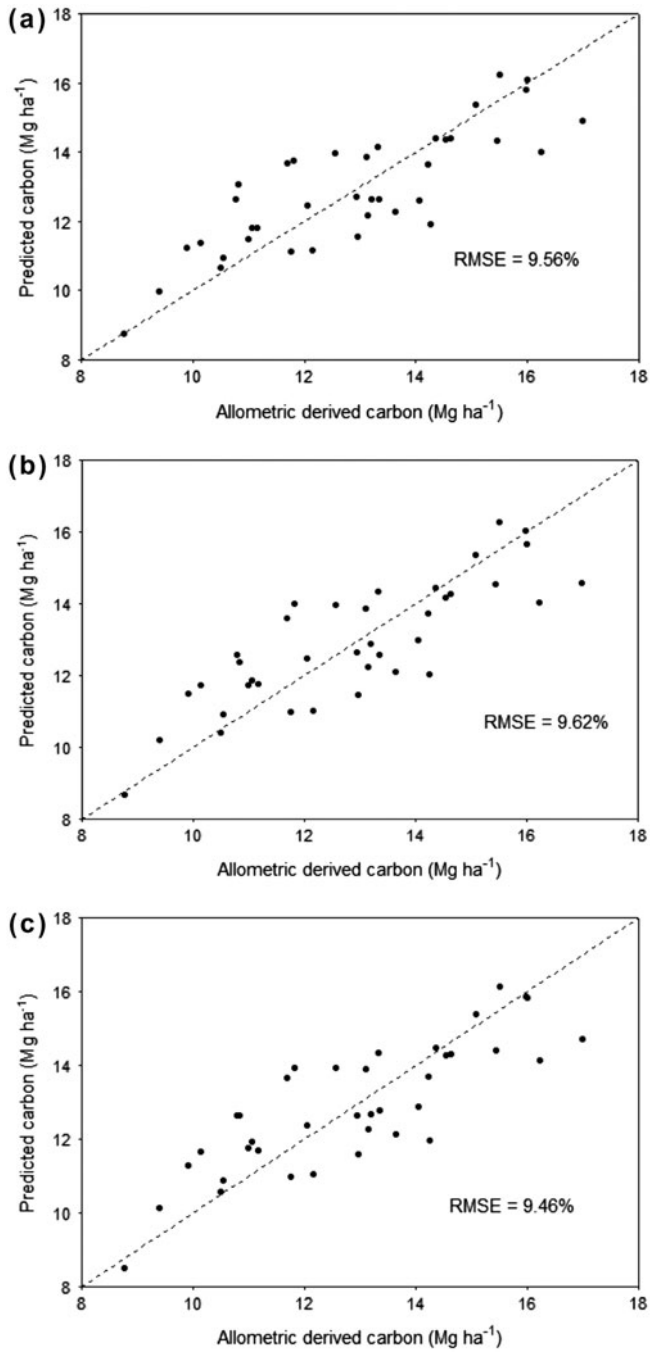
Figure 5.   Relationships between measured carbon and predicted carbon as predication indices (a = SR, b = NDVI, c = SAVI). The dotted line is a 1:1 line. The 1:1 line shows how closely the models predicted carbon stocks.
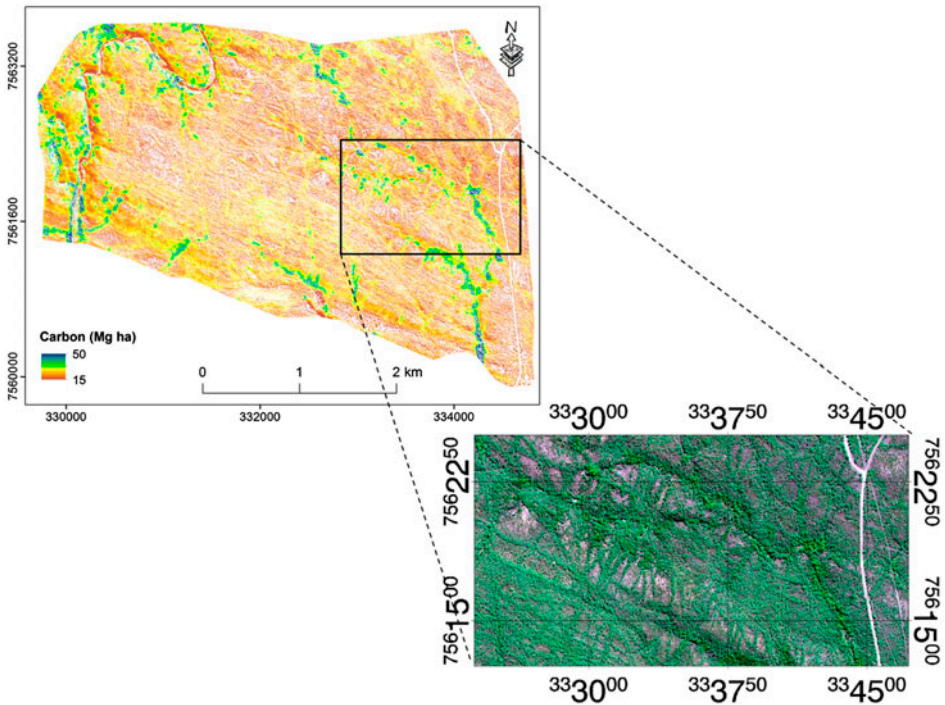
Figure 6. Spatial variation in carbon stocks as estimated by the SR and reflectance in the red edge band (white spaces are bare areas including roads).

regard, additional information on tree height acquired from Light Detection and Ranging (LIDAR) may be important to achieve higher accuracy.

This study differs from previous studies in three main ways. Firstly, studies that have used vegetations to estimate biomass or carbon in African savanna have used vegetation indices as only explanatory variable in aboveground biomass estimations in the African savanna. However, in this study, we estimated carbon stocks from vegetation indices and RE band derived from high spatial resolution satellite imagery with very low error margins. Thus, it is important to note that integrating vegetation indices and reflectance in the RE band derived from high resolution improved carbon predictions compared previous studies. The use of the RE band has mainly being limited to hyperspectral imagery analysis, especially grass/crop biomass and biochemical (nitrogen) analysis. Its application in broadband multispectral imagery has been limited. This is mainly attributed to the fact that many broadband satellite borne imagery like Landsat do not have RE band. Moreover, the vegetation indices are often been derived from medium to low spatial resolution satellite imagery data such as Landsat, MODIS and AHVRR. These factors have resulted in weak relationships, high errors and uncertainties (du Plessis 1999; Samimi & Kraus 2004; Wessels et al. 2006). Secondly, studies conducted in the African savanna focused on AGB (du Plessis 1999; Samimi & Kraus 2004; Mutanga & Rugege 2006) and very few proceed to estimate carbon from AGB, yet carbon is an important dendrometric variable that has direct meaning to the science of climate change Finally, unlike previous studies that only determined the relationships

between spectral bands, vegetation indices and tree structural attributes in African savannas we mapped the spatial variation in carbon stocks at a fine spatial scale with a low RMSE. Again, we find this especially important in African savannas woodlands where tree cover is low, thus making high spatial resolution satellite imagery an excellent alternative to delineating spatial variability in carbon. However, it would be useful to test the applicability of these models in independent study sites to observe whether the form of remotely sensed models of carbon are consistent and can be improved further. Nevertheless, we make a claim that this finding provides an opportunity to modelling carbon storage in dry forests such as the savanna woodlands of Southern Africa.

5.   Conclusion

The main objective of this study was to test whether the inclusion of reflectance in the RE band as a covariate to conventional vegetation indices could improve estimations of forest carbon stocks estimations in savanna dry forests.

From the results of this study, we conclude that:

(1) The inclusion of reflectance in the RE band as an covariate to vegetation indices improve the prediction accuracy of carbon estimation in savanna woodlands. Vegetation indices alone explained between 45 and 63% variation in carbon stocks with a RMSE of between 10.3 and 12.9%. With the inclusion of the red edge the explained variance varied between 68 and 70% with the RMSE decreasing to between 9.56 and 10.1%.
(2) Regression models developed based on vegetation indices and reflectance in the RE band can be successfully used to map the spatial variation in carbon stocks in savanna dry forests.

We finally conclude that the RE band is important in estimating and mapping spatial variability in carbon stocks with relatively high levels of accuracy in savanna woodlands of Southern Africa. The findings of these results are critical in selection of sensitive bands of hyperspectral remote sensors in quantifying carbon stocks. We suggest that further studies could aim to include important dendrometric variable such as tree height estimated using LIDAR to check if further improvements can be achieved.

Disclosure statement

References

Abbot P, Lowore J, Werren M. 1997. Models for the estimation of single tree volume in four Miombo woodland types. Forest Ecol Manage. 97:25–37.
Bernstein LS, Adler-Golden SM, Sundberg RL, Levine RY, Perkins TC, Berk A, Ratkowski AJ, Felde G, Hoke ML. 2005b. Validation of the QUick Atmospheric Correction (QUAC) algorithm for VNIR-SWIR multi- and hyperspectral imagery. Paper presented at: SPIE proceedings, algorithms and technologies for multispectral, hyperspectral, and ultraspectral imagery; Bellingham.
Brauner N, Shacham M. 1998. Identifying and removing sources of imprecision in polynomial regression. Math Comput Simul. 48:75–91.

Brown S. 1997. Estimating biomass and biomass change of tropical forests: a Primer. (FAO forestry paper – 134). Rome: FAO.

Cho MA, Skidmore A, Corsi F, van Wieren SE, Sobhan I. 2007. Estimation of green grass/herb biomass from airborne hyperspectral imagery using spectral indices and partial least squares regression. Int J Appl Earth Obs Geoinf. 9:414–424.

De Gier A. 2003. A new approach to woody biomass assessment in woodlands and shrublands. In: Roy P, editor. Geoinformatics for tropical ecosystems. Calcutta: Asian Association of Remote Sensing; p. 161–198.

du Plessis WP. 1999. Linear regression relationships between NDVI, vegetation and rainfall in Etosha National Park, Namibia. J Arid Environ. 42:235–260.

Eisfelder C, Kuenzer C, Dech S. 2011. Derivation of biomass information forsemi-arid areas using remote-sensing data. Int J Remote Sens. 33:1–48.

Filella I, Penuelas J. 1994. The red edge position and shape as indicators of plant chlorophyll content, biomass and hydric status. Int J Remote Sens. 15:1459–1470.

Gara TW, Murwira A, Chivhenge E, Dube T, Bangira T. 2014. Estimating wood volume from canopy area in deciduous woodlands of Zimbabwe. South Forests: J Forest Sci. 76:237–244.

Gibbs HK, Brown S, Niles JO, Foley JA. 2007. Monitoring and estimating tropical forest carbon stocks: making REDD a reality. Environ Res Lett. 2:1–13.

Gschwantner T, Schadauer K, Vidal C, Lanz A, Tomppo E, di Cosmo L, Robert N, Duursma Englert, Lawrence M. 2009. Common tree definitions for national forest inventories in Europe. Silva Fennica. 43:303–321.

Henry M, Picard N, Trotta C, Manlay RJ, Valentini R, Bernoux M, Saint-André L. 2011. Estimating tree biomass of sub-Saharan African forests: a review of available allometric equations. Silva Fennica. 45:477–569.

Huete AR. 1988. A soil adjusted vegetation index (SAVI). Int J Remote Sens. 9:295–309.

ILUA. 2008. Integrated land use assement 2005–2008 Republic of Zambia. Lusaka: Zambia Forestry Department.

IPCC. 2003. Good practice guidance for land use, land-use change and forestry. National Greenhouse Gas Inventories Programme. Hayama: IPCC; p. 295.

Jordan CF. 1969. Derivation of leaf-area index from quality of light on the forest floor. Ecology. 50:663–666.

Ketterings QA, Coe R, van Noordwijk M, Ambagau Y, Palm CA. 2001. Reducing uncertainty in the use of allometric biomass equations for predicting above-ground tree biomass in mixed secondary forests. Forest Ecol Manage. 146:199–209.

Legendre P. 1993. Spatial autocorrelation: trouble or new paradigm? Ecology. 74:1659–1673.

Lu D. 2006. The potential and challenge of remote sensing-based biomass estimation. Int J Remote Sens. 27:1297–1328.

Mutanga O, Adam E, Cho MA. 2012. High density biomass estimation for wetland vegetation using WorldView-2 imagery and random forest regression algorithm. Int J Appl Earth Obs Geoinf. 18:399–406.

Mutanga O, Rugege D. 2006. Integrating remote sensing and spatial statistics to model herbaceous biomass distribution in a tropical savanna. Int J Remote Sens. 27:3499–3514.

Mutanga O, Skidmore AK. 2007. Red edge shift and biochemical content in grass canopies. ISPRS J Photogramm Remote Sens. 62:34–42.

Muukkonen P, Heiskanen J. 2005. Estimating biomass for boreal forests using ASTER satellite data combined with standwise forest inventory data. Remote Sens Environ. 99:434–447.

Muukkonen P, Heiskanen J. 2007. Biomass estimation over a large area based on standwise forest inventory data and ASTER and MODIS satellite data: a possibility to verify carbon inventories. Remote Sens Environ. 107:617–624.

Northup BK, Zitzer SF, Archer S, McMurtry CR, Boutton TW. 2005. Above-ground biomass and carbon and nitrogen content of woody species in a subtropical thornscrub parkland. J Arid Environ. 62:23–43.

Rahman MM, Csaplovics E, Koch B. 2008. Satellite estimation of forest carbon using regression models. Int J Remote Sens. 29:6917–6936.

Rawlings JO, Pantula SG, Dickey DA. 1998. Applied regression analysis. 2nd ed. New York (NY): Springer.

Samimi C, Kraus T. 2004. Biomass estimation using Landsat-TM and -ETM+. Towards a regional model for Southern Africa? GeoJournal. 59:177–187.

Tucker CJ. 1979. Red and photographic infrared linear combinations for monitoring vegetation. Remote Sens Environ. 8:127–150.

Turpie KR. 2013. Explaining the spectral red-edge features of inundated marsh vegetation. J Coastal Res. 29:1111–1117.

Van TK, Rayachhetry MB, Center TD. 2000. Estimating above-ground biomass of Melaleuca quinquenervia in Florida, USA. J Aquat Plant Manage. 38:62–67.

Verbesselt J, Somers B, van Aardt J, Jonckheere I, Coppin P. 2006. Monitoring herbaceous biomass and water content with SPOT VEGETATION time-series to improve fire risk assessment in savanna ecosystems. Remote Sens Environ. 101:399–414.

Wessels KJ, Prince SD, Zambatis N, MacFadyen S, Frost PE, Zyl DV. 2006. Relationship between herbaceous biomass and 1-km2 advanced very high resolution radiometer (AVHRR) NDVI in Kruger National Park, South Africa. Int J Remote Sens. 27:951–973.

Williams CA, Hanan NP, Neff JC, Scholes RJ, Berry J, Denning AS, Baker DF. 2007. Africa and the global carbon cycle. Carbon Balance Manage. 2:1–13.

Zianis D, Muukkonen P, Mäkipää R, Mencuccini M. 2005. Biomass and stem volume equations for tree species in Europe. Silva Fennica Monographs. 4, p. 63. Helsinki: The Finish Society of Forest Science.